

Evaluation of sensorless VF-MRAS and FOC-MRAS of IM electrical drive system

Moustapha Diop, Abdoulaye Kebe, Ibrahima Gueye

Department STI, Ecole Normale Supérieure d'Enseignement Technique et Professionnel, Université Cheikh Anta Diop, Dakar, Senegal
Laboratoire L3EPI, Ecole Supérieure Polytechnique, Université Cheikh Anta Diop, Dakar, Sénégal

Article Info

Article history:

Received Jul 20, 2024

Revised Dec 26, 2024

Accepted Jan 19, 2025

Keywords:

Field-oriented control

Induction motor

MRAS

Scalar V/f

Sensorless control

ABSTRACT

This paper evaluates the performance of sensorless vector and scalar control methods, namely field-oriented control-based model reference adaptive system (FOC-MRAS) and voltage frequency-based model reference adaptive system (VF-MRAS), applied to an induction motor (IM) driven by a space vector modulation inverter. In motorized systems, conventional control methods use mechanical sensors, which can be cumbersome and costly. To overcome these limitations, sensorless control techniques based on speed estimation have been introduced. In this paper, MRAS-based sensorless speed control for IM drives using rotor flux is used. This adaptive system uses a reference model based on rotor flux and implements closed-loop control. The estimated speed derived from the current and voltage models is compared to the desired speed and adjusted by the proportional-integral (PI) controllers. The performances of the approaches are evaluated in terms of speed regulation and minimization of electromagnetic torque and rotor flux ripples, through a comparative analysis of sensor and sensorless controls under various operating conditions, including variable loads and speed reversal. The simulation results obtained, using consistent criteria for both methods, confirm the effectiveness of sensorless control.

This is an open access article under the [CC BY-SA](#) license.



Corresponding Author:

Moustapha Diop

Department STI, Ecole Normale Supérieure d'Enseignement Technique et Professionnel

Université Cheikh Anta Diop

Dakar, Senegal

Email: moustapha17.diop@ucad.edu.sn

1. INTRODUCTION

Induction motors are the most widely used variable speed drives because of their robustness, reliability, simplicity and straightforward control process [1]-[5]. However, to achieve high performance with the induction motors (IMs), it is necessary to select an effective control strategy tailored to specific applications. For induction motor (IM) control, several techniques have been proposed, such as traditional direct torque control (DTC), scalar control (V/f), and field-oriented control (FOC) [6]. The DTC is characterized by good dynamic torque response and easy to implement. However, both torque and electromagnetic flux exhibit ripples [7]. For the FOC, it is distinguished by its good dynamic response [8]. It maintains efficiency over a wide speed range and takes into account the load torque variations. As for scalar control, it is simple, less costly, allows slow speed variation and is easy to implement, but it exhibits poor dynamic performance and is typically used in low-cost, and low-performance system drives.

The above-mentioned controls have advantages and limitations depending on the application. As the ability to operate at variable speed is a fixed objective in this work, the FOC and voltage frequency (VF) controls are used with the aim of improving their performance by exploring alternative implementation strategies. However, efficient execution of these closed-loop strategies requires speed information. To this end, the use of mechanical sensors has often been necessary. However, their use presents certain limitations, such as increased device cost, reduced reliability and low noise immunity. For this reason, recent research has largely focused on sensorless drives.

The sensorless control enables speed to be reconstructed from the IM model. Several techniques are used, including open-loop technique, sliding mode observer (SMO), extended Kalman filter observer, and model reference adaptive systems (MRAS) observer [9]–[13]. Open-loop estimators have always attracted attention due to their simplicity, but they exhibit low robustness [14]. The Kalman method is widely used for flux and speed estimation [15]–[17]. Although the estimated variables are well filtered, the method is often impractical at low speeds, sensitive to parameter variations, and difficult to implement. As for the SMO, it is robust and simple to implement. However, its use is limited by oscillations that can lead to instability, and computational complexity is significantly increased. The Luenberger technique yields good results but is sensitive to disturbances and parameter variations, and is also challenging to synthesize [18]. For the MRAS technique, widely used for estimating motor speed or motor resistance, it is based on comparing a reference model that is independent of speed to an adjustable adaptive model that depends on speed [19]. The error is corrected by an adaptation mechanism using a proportional-integral (PI) controller that determines the estimated motor speed [20]. This method provides good results, is straightforward to implement has good accuracy and requires less computational effort compared to the mentioned estimator techniques [21].

In this work, the flux-based MRAS technique is adopted for speed estimation applied to FOC and VF drives. In this respect, this paper proposes an alternative methodology for estimating speed via MRAS of a three-phase IM driven by a space vector modulation (SVM) voltage source inverter (VSI). The SVM strategy is employed to achieve reduced harmonic distortion, and minimized switching losses [22]–[24]. The proposed control methods are evaluated in terms of speed regulation, as well as reductions in torque and rotor flux ripple. A comparative study of sensor and sensorless control strategies was conducted under different operating conditions.

This research is divided into four sections. Following an introduction in section 1, section 2 presents the mathematical models of the drive system components and the proposed control strategies. Section 3 presents and discusses the simulation results. Finally, the paper concludes in section 4.

2. MATERIALS AND METHOD

In this paper, the performances of sensorless FOC and VF controls, based on the closed-loop MRAS technique are studied. The drive system consists of a three-phase IM driven by a SVM VSI. The IM models in (d-q) and (alpha-beta) reference frames are developed initially. This model will be used to establish equations for estimating speed using the MRAS method. The parameters of the controllers used are calculated to achieve fast adaptive loop that is independent of load torque variation. The models and control strategies are then implemented and simulated using the MATLAB-Simulink software tool under various load conditions.

2.1. Induction motor modeling

In this work, the dq and α, β models are used. The dq model described by (1)–(4) allows for establishing conventional controls, while the α, β model is essential for sensorless control. The dq model can be subsequently transformed into stationary coordinates (α, β) using the inverse Park transformation.

$$v_{ds} = R_s i_{ds} + L_s \left(1 - \frac{L_m^2}{L_r L_s} \right) \frac{di_{ds}}{dt} + \frac{L_m}{L_r} \frac{d\phi_{dr}}{dt} - L_s \left(1 - \frac{L_m^2}{L_r L_s} \right) \omega_s i_{qs} - \omega_s \frac{L_m}{L_r} \phi_{qr} \quad (1)$$

$$v_{qs} = R_s i_{qs} + L_s \left(1 - \frac{L_m^2}{L_r L_s} \right) \frac{di_{qs}}{dt} + \frac{L_m}{L_r} \frac{d\phi_{qr}}{dt} - L_s \left(1 - \frac{L_m^2}{L_r L_s} \right) \omega_s i_{ds} + \omega_s \frac{L_m}{L_r} \phi_{dr} \quad (2)$$

$$\phi_{dr} = -T_r \frac{d\phi_{dr}}{dt} + T_r \omega_r \Phi_{qr} + L_m i_{ds} \quad \phi_{qr} = -T_r \frac{d\phi_{qr}}{dt} - T_r \omega_r \Phi_{dr} + L_m i_{qs} \quad (3)$$

$$J \frac{d\Omega}{dt} = T_{em} - T_L - f_r \Omega \quad T_{em} = p \frac{L_m}{L_r} (\phi_{dr} i_{qs} - i_{ds} \phi_{qr}) \quad (4)$$

2.2. SVM inverter modeling

The diagram of the VSI comprises three branches and six switches whose switching depends is determined by the SVM scheme depicted in Figure 1. With the SVM, the VSI require a voltage vector space, i.e., 8 possible switching states that are then transformed into voltage vectors in α, β frame corresponding to well-defined sequences [25]. Regarding the VSI model, only six of the eight voltage vectors (001), (101), (100), (110), (010), and (011) are active as control elements. The vectors (000) and (111) are null. The active switching states, the line voltages, and the two-phase voltage levels v_α and v_β are summarized in Table 1.

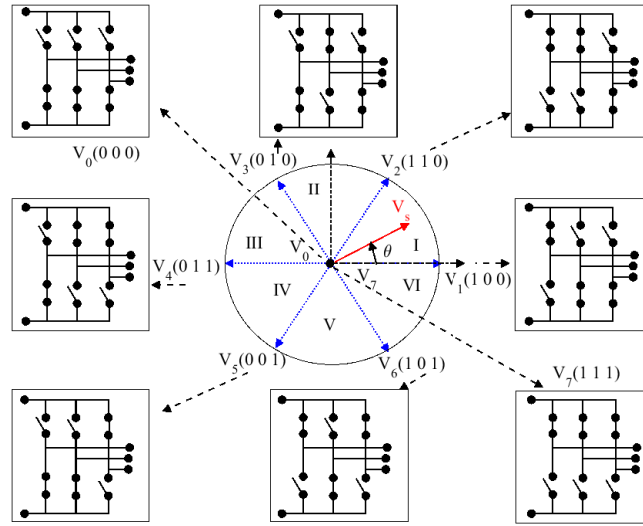


Figure 1. General diagram of SVM inverter

Table 1. Switching states and voltages table

States	v_a	v_b	v_c	v_α	v_β
000	0	0	0	0	0
100	$2V_{dc}/3$	$-V_{dc}/3$	$-V_{dc}/3$	$2V_{dc}/3$	0
110	$V_{dc}/3$	$V_{dc}/3$	$-2V_{dc}/3$	$V_{dc}/3$	$\sqrt{3}V_{dc}/3$
010	$-V_{dc}/3$	$2V_{dc}/3$	$-V_{dc}/3$	$-V_{dc}/3$	$\sqrt{3}V_{dc}/3$
011	$-2V_{dc}/3$	$V_{dc}/3$	$V_{dc}/3$	$-2V_{dc}/3$	0
001	$-V_{dc}/3$	$-V_{dc}/3$	$2V_{dc}/3$	$-V_{dc}/3$	$-\sqrt{3}V_{dc}/3$
101	$V_{dc}/3$	$-2V_{dc}/3$	$V_{dc}/3$	$V_{dc}/3$	$-\sqrt{3}V_{dc}/3$
111	0	0	0	0	0

2.3. Speed observer based on MRAS

The principle for controls relies on comparing reference model (RM) and adaptive model (AM), as depicted in Figure 2 [19]. The RM corresponds to the rotor flux calculated from current and voltage feedback, while the AM corresponds to the rotor flux derived from rotor equations. The error between these models is used to drive an appropriate adaptation mechanism using a PI controller that generates the estimated speed [20]. Rotor fluxes (Φ_α^* , Φ_β^*) of the RM and rotor fluxes of adaptive model ($\hat{\phi}_\alpha$, $\hat{\phi}_\beta$) are given by:

$$\frac{d\phi_{\alpha r}^*}{dt} = \frac{L_r}{L_m} \left(v_{\alpha s} - R_s i_{\alpha s} - L_s \left(1 - \frac{L_m^2}{L_r L_s} \right) \frac{di_{\alpha s}}{dt} \right) \quad (5)$$

$$\frac{d\phi_{\beta r}^*}{dt} = \frac{L_r}{L_m} \left(v_{\beta s} - R_s i_{\beta s} - L_s \left(1 - \frac{L_m^2}{L_r L_s} \right) \frac{di_{\beta s}}{dt} \right) \quad (6)$$

$$\frac{d\hat{\phi}_{\alpha r}}{dt} = -\frac{1}{T_r} \hat{\phi}_{\alpha r} + \frac{L_m}{T_r} i_{s\alpha} - \omega \hat{\phi}_{\beta r} \quad (7)$$

$$\frac{d\hat{\phi}_{\beta r}}{dt} = -\frac{1}{T_r} \hat{\phi}_{\beta r} + \frac{L_m}{T_r} i_{s\beta} + \omega \hat{\phi}_{\alpha r} \quad (8)$$

$v_{\alpha s}$ and $v_{\beta s}$ denote the stator voltages, while $i_{\alpha s}$ and $i_{\beta s}$ represent the stator currents, all expressed in the $\alpha\beta$ frame, which are used as feedback inputs to the motor control system as represented in Figure 2.

According to the error signals used as input to the PI controller, the estimated speed is determined. It can be expressed as (9).

$$\omega = \epsilon \left(k_1 + \frac{k_2}{s} \right) = \left(k_1 + \frac{k_2}{s} \right) \left(\hat{\phi}_\alpha \phi_\beta^* - \hat{\phi}_\beta \phi_\alpha^* \right) \quad (9)$$

The PI controller gains k_1 and k_2 are tuned based on the MRAS closed-loop transfer function (CLTF), obtained by linearizing the adaptation model. Assuming perfect flux orientation with constant flux and current magnitudes ($\phi_\alpha^* = \Phi_r$ and $\phi_\beta^* = 0$), the (10) gives the linearized expression of the error.

$$\delta\epsilon = \Phi_\beta^* \delta\hat{\Phi}_\alpha + \hat{\Phi}_\alpha \delta\Phi_\beta^* - \hat{\Phi}_\beta \delta\Phi_\alpha^* - \Phi_\alpha^* \delta\hat{\Phi}_\beta = -\Phi_\alpha^* \delta\hat{\Phi}_\beta \quad (10)$$

The linearization of the adaptive model expressions gives as (11).

$$s \delta\hat{\Phi}_\alpha = -\frac{1}{T_r} \delta\hat{\Phi}_\alpha + \omega \delta\hat{\Phi}_\beta \quad s \delta\hat{\Phi}_\beta = -\frac{1}{T_r} \delta\hat{\Phi}_\beta - \omega \delta\hat{\Phi}_\alpha + \hat{\Phi}_\alpha \delta\omega \quad (11)$$

The substitution of the previous equations gives as (12).

$$\delta\hat{\Phi}_\beta = -\frac{\Phi_r(T_r s + 1)}{(T_r s + 1)^2 + (\omega T_r)^2} \delta\omega \quad (12)$$

Since $\delta\epsilon = -\phi_\alpha^* \delta\hat{\Phi}_\beta$, the open-loop transfer function is as (13).

$$G_0(s) = \frac{\delta\epsilon}{\delta\omega} = -\Phi_r^2 \frac{(T_r s + 1)}{(T_r s + 1)^2 + (\omega T_r)^2} \quad (13)$$

Using the PI controller, the transfer function $G_f(s)$ is expressed. Pole-placement-tuned PI controllers gains are calculated where ζ and $\omega_{n_{est}}$ are the damping coefficient and the natural frequency.

$$G_f(s) = \frac{(k_1 s + k_2) \phi_r^2}{s^2 + \left(\frac{1}{T_r} + \Phi_r^2 k_1 \right) s + k_2 \phi_r^2} \quad (14)$$

$$k_1 = \frac{2\zeta T_r \omega_{n_{est}} - 1}{T_r \Phi_r^2} \quad k_2 = \frac{\omega_{n_{est}}^2}{\Phi_r^2} \quad (15)$$

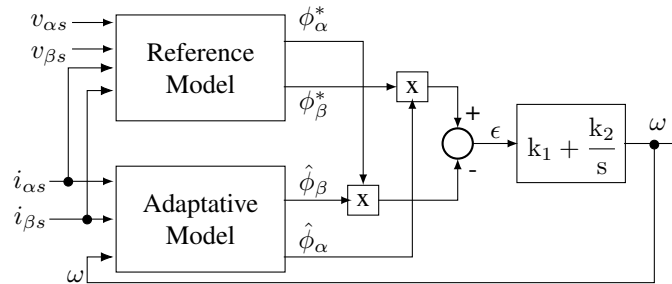


Figure 2. MRAS structural diagram

2.4. VF-MRAS

Scalar control aims to keep the magnetic flux constant at its maximum value by keeping the voltage/frequency ratio constant and boosting it to minimize the voltage drop across the stator resistance at low speed. For scalar control, torque is controlled by slip variation and its expression is given by (16). The control system of the closed-loop V/f-MRAS depicted in Figure 3 includes an outer-loop estimator to determine the

motor speed (ω). According to the scheme, the estimated speed is compared with a reference speed (ω^*). The resulting error is fed into the PI speed controller, which calculates a slip angular speed that is then added to the estimated motor speed to derive the frequency. Figure 4 shows the synthesis of speed corrector. The controller gains can be calculated using (17).

$$T_{em-max} = \frac{3p}{2R_r} \frac{L_m^2}{L_s^2} \frac{V_n^2}{\omega_n^2} \times \omega_{sl} \quad (16)$$

$$k_p = \frac{2R_r L_s^2 \omega_n^2}{3p L_m^2 V_n^2} (2J_{ki} \zeta \omega_c - f_r) \quad k_i = \frac{2R_r L_s^2 \omega_n^2}{3p L_m^2 V_n^2} J \omega_c^2 \quad (17)$$

2.5. FOC-MRAS

For the FOC technique, the rotor flux and motor torque are controlled respectively by the direct and the quadrature current components. For determining the rotor position, the sensorless MRAS technique is used to estimate rotor position information in real time. Figure 5 illustrates the FOC-MRAS control scheme.

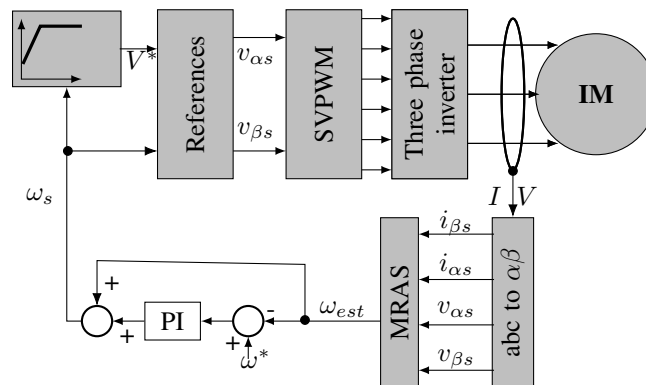


Figure 3. Synoptic diagram of the proposed V/f-MRAS strategy

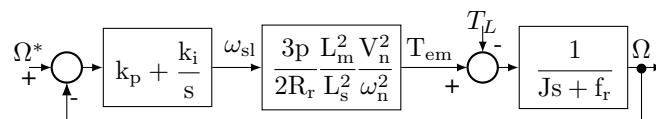


Figure 4. Synthesis of the speed corrector for scalar control

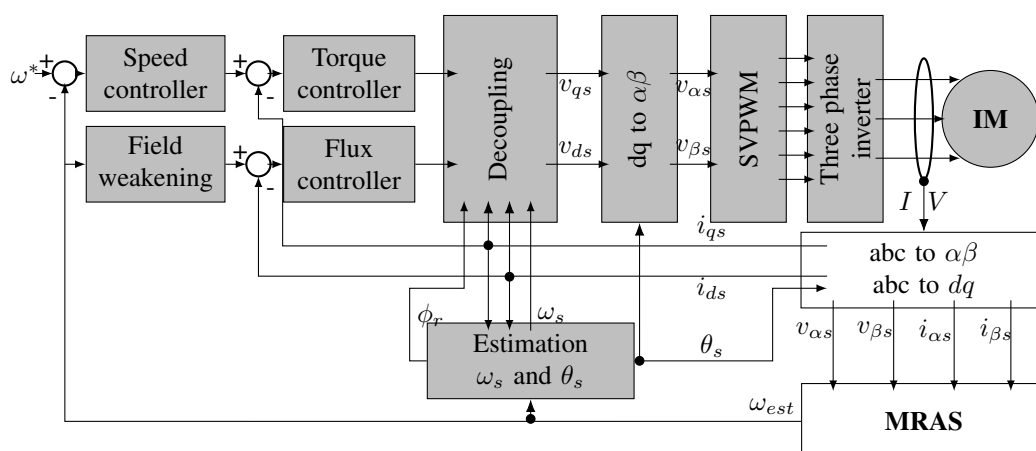


Figure 5. Synoptic diagram of the proposed FOC-MRAS strategy

The control structure consists of an outer speed controller in a closed-loop and a series of inner current controllers. On the basis of a cascade control, the current controllers dynamics is sufficiently fast with respect to speed loop. The diagrams is represented in Figure 6. The controller gains can be calculated using (18).

$$k_{i\Omega} = J\omega_{c\Omega}^2 \quad k_{p\Omega} = 2J\zeta\omega_{c\Omega} - f_r \quad (18)$$

ζ is damping coefficient, and $\omega_{c\Omega}$ the own pulsation.

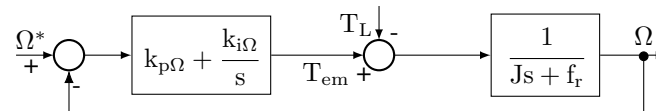


Figure 6. Synthesis of the speed corrector for FOC control

3. RESULTS AND DISCUSSION

The FOC-MRAS and V/f-MRAS controls are evaluated through simulation using MATLAB/Simulink and a 2.2 kW IM in this section. The performances are assessed by comparing the results with those obtained from sensor-based controls under various operating conditions. The first test was conducted to verify the performance in terms of reference speed tracking. The results are presented in Figures 7 to 11. For each case, the reference speed was set to 314 rad/s, with a load torque of 3.7 Nm (half load) applied at $t = 3$ s and the rated load of 7.37 Nm at $t = 5$ s. A second test was performed to assess the strategies under reverse operation mode. According to results represented respectively in Figures 8 and 11, the torque follows the variation of the load with a slight offset due to the mechanical parameters of the motor, and exhibits noise associated to fluctuations in the estimated speed. Additionally, the magnetic flux is properly oriented towards the direct axis.

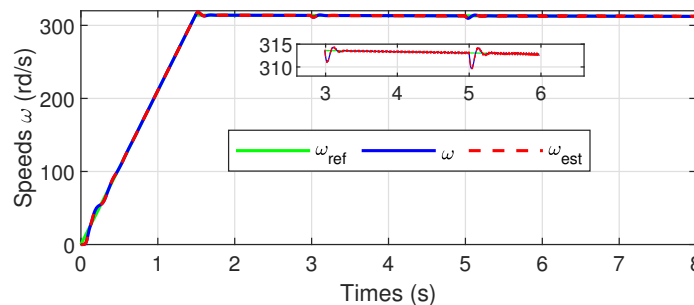


Figure 7. Reference, real, and estimated rotor speeds VF-MRAS

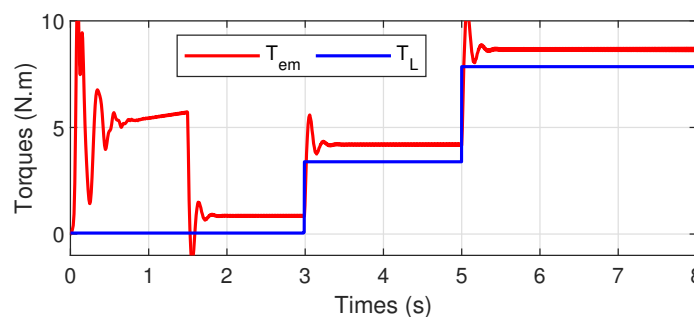


Figure 8. Load and motor torques VF-MRAS

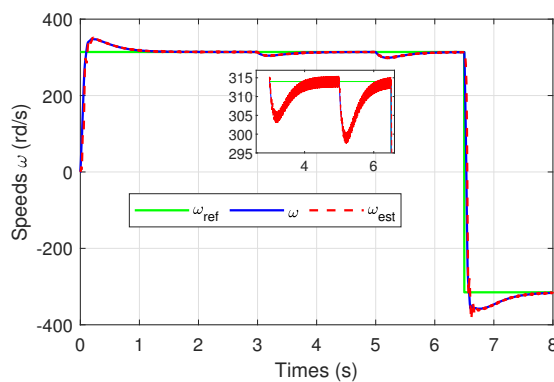


Figure 9. Reference, real, and estimated rotor speeds FOC-MRAS

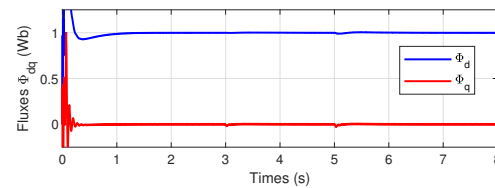


Figure 10. Rotor fluxes FOC-MRAS

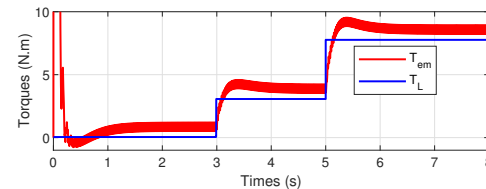


Figure 11. Load and motor torques FOC-MRAS

To test the robustness of the sensorless strategies against disturbances, the system is simulated using a variable load profile. The measured, estimated, and reference speeds are shown in the Figures 7 and 9. The results show that the proposed MRAS speed estimator enables accurate tracking of the actual motor speed, with a fast response time. The zooms around the instants at 3 s and 5 s, when loads are applied, demonstrate accurate tracking that reflects the effectiveness and robustness of the control in rejecting disturbances, despite proportional variations in the applied load. Moreover, the results show the speed estimation error. It indicates the instantaneous difference between the actual speeds and the estimated speeds, which is almost zero. To further evaluate the strategy, at $t = 6.5$ s, a reversal of rotation direction followed by a speed reference of +314 rad/s and -314 rad/s is performed to test the performance in these regimes. Figure 9 shows similar behavior, with a slight delay observed in the transient phases. Thus, the MRAS technique enables accurate speed estimation in these regimes, ensuring good agreement with the reference and near-perfect approximation with the estimated speed.

In summary, the figures presented above illustrate a series of simulation results aimed at evaluating the performance of the FOC-MRAS and VF-MRAS controls. Tests include load variations, reversals of rotation direction, and detailed analyses of motor flux and torque. The results show that the estimated speed using MRAS control enables accurate tracking of the motor's actual speed, with fast response and good robustness to disturbances. Overall, the control strategies demonstrate an effective ability to maintain motor speed close to reference despite varying load and operating conditions. The strategies exhibit excellent reference tracking, and the speed transient regime is characterized by fast response times without significant overshoot.

4. CONCLUSION

The conclusion of this paper summarizes the validation and benefits of a sensorless vector and scalar IM drive based on the MRAS method with speed estimation. The proposed control scheme is simulated under different operation conditions, including load variation, and rotation inversion. Overall, the simulation results highlights the robustness and improved performance of the proposed control strategies. The results emphasize enhanced speed tracking, instantaneous speed estimation, and reduced flux and torque ripples. The developed control schemes show promising potential for practical applications, as sensorless induction motor control integrated with speed estimation mitigates the disadvantages associated with speed sensors, such as reduced reliability, noise sensitivity, increased cost, weight, and system complexity of the drive system.

FUNDING INFORMATION

The authors declare that no funding was received for this research.

AUTHOR CONTRIBUTIONS STATEMENT

This journal uses the Contributor Roles Taxonomy (CRediT) to recognize individual author contributions, reduce authorship disputes, and facilitate collaboration.

Name of Author	C	M	So	Va	Fo	I	R	D	O	E	Vi	Su	P	Fu
Moustapha Diop	✓	✓	✓	✓	✓	✓	✓		✓	✓	✓	✓	✓	✓
Abdoulaye Kebe		✓				✓			✓	✓	✓		✓	✓
Ibrahima Gueye		✓	✓	✓		✓			✓		✓		✓	✓

C : Conceptualization

M : Methodology

So : Software

Va : Validation

Fo : Formal Analysis

I : Investigation

R : Resources

D : Data Curation

O : Writing - Original Draft

E : Writing - Review & Editing

Vi : Visualization

Su : Supervision

P : Project Administration

Fu : Funding Acquisition

CONFLICT OF INTEREST STATEMENT

The authors declare that they have no known competing financial interests or personal relationships that could have appeared to influence the work reported in this paper.

DATA AVAILABILITY

Data availability is not applicable to this paper as no new data were created or analyzed in this study.




REFERENCES

- [1] A. Sahu, K. B. Mohanty, R. N. Mishra, "Development and experimental realization of an adaptive neural-based discrete model predictive direct torque and flux controller for induction motor drive," *Applied Soft Computing*, vol. 108, Sep. 2021, doi: 10.1016/j.asoc.2021.107418.
- [2] A. Gundogdu, H. Kizmaz, R. Celikel, and M. Yilmaz, "Speed sensorless adaptive power control for photovoltaic-fed water pump using extended Kalman Bucy filter," *Energy Reports*, vol. 10, pp. 1785-1795, 2023, doi: 10.1016/j.egyr.2023.08.036.
- [3] K. Saad, K. Abdellah, H. Ahmed, and A. Iqbal, "Investigation on SVM-backstepping sensorless control of five-phase open-end winding induction motor based on model reference adaptive system and parameter estimation," *Engineering Science and Technology, an International Journal*, vol. 22, no. 4, pp. 1013-1026, 2019, doi: 10.1016/j.jestch.2019.02.008.
- [4] S. A. Bernarz and M. Dybkowski, "Estimation of the induction motor stator and rotor resistance using active and reactive power based model reference adaptive system estimator," *Applied Sciences*, vol. 9, no. 23, 2019, doi: 10.3390/app9235145.
- [5] H. Hadla and F. Santos, "Performance comparison of field-oriented control, direct torque control, and model-predictive control for SynRMs," *Chinese Journal of Electrical Engineering*, vol. 8, no. 1, pp. 24-37, Mar. 2022, doi: 10.23919/CJEE.2022.00000.
- [6] N. El Ouanjli *et al.*, "Improved twelve sectors DTC strategy of induction motor drive using backstepping speed controller and P-MRAS stator resistance identification-design and validation," *Alexandria Engineering Journal*, vol. 80, pp. 358-371, 2023, doi: 10.1016/j.aej.2023.08.077.
- [7] Y. Ren, R. Wang, S. J. Rind, P. Zeng, and L. Jiang, "Speed sensorless nonlinear adaptive control of induction motor using combined speed and perturbation observer," *Control Engineering Practice*, vol. 123, 105166, 2022, doi: 10.1016/j.conengprac.2022.105166.
- [8] Y. Zahraoui, A. Bennassar, M. Akherraz, and A. Essalmi, "Indirect vector control of induction motor using an extended Kalman observer and fuzzy logic controllers," *2015 3rd International Renewable and Sustainable Energy Conference (IRSEC)*, Morocco, Dec. 2015, doi: 10.1109/IRSEC.2015.7455046.
- [9] F. Z. Latrech, A. B. Rhouma, and A. Khedher, "FPGA implementation of a robust DTC-SVM based sliding mode flux observer for a double star induction motor: Hardware in the loop validation," *Microelectronics Reliability*, vol. 150, 2023, doi: 10.1016/j.microrel.2023.115118.
- [10] J. Gamazo-Real, V. Martínez-Martínez, and J. Gomez-Gil, "ANN-based position and speed sensorless estimation for BLDC motors," *Measurement*, vol. 188, 2022, doi: 10.1016/j.measurement.2021.110602.
- [11] C. U. Reddy, K. K. Prabhakar, A. K. Singh, and P. Kumar, "Speed estimation technique using modified stator current error-based MRAS for direct torque controlled induction motor drives," in *IEEE Journal of Emerging and Selected Topics in Power Electronics*, vol. 8, no. 2, pp. 1223-1235, Jun. 2020, doi: 10.1109/JESTPE.2019.2901523.
- [12] A. Boyar, E. Kabalci, and Y. Kabalci, "Sensorless speed controller of an induction motor with MRAS-based model predictive control," *Computers and Electrical Engineering*, vol. 118, 2024, doi: 10.1016/j.compeleceng.2024.109350.
- [13] M. Touam, M. Chenafa, S. Chekroun, and R. Salim, "Sensorless nonlinear sliding mode control of the induction machine at very low speed using FM-MRAS observer," *International Journal of Power Electronics and Drive Systems*, vol. 12, no. 4, pp. 1987-1998, doi: 10.11591/ijpeds.v12.i4.pp1987-1998.
- [14] F. Lima, W. Kaiser, I. N. da Silva, and A. A. A. de Oliveira, "Open-loop neuro-fuzzy speed estimator applied to vector and scalar induction motor drives," *Applied Soft Computing*, vol. 21, pp. 469-480, 2014, doi: 10.1016/j.asoc.2014.03.044.
- [15] J. Li, "Model predictive control for extended Kalman filter based speed sensorless induction motor drives," *2016 IEEE Applied Power Electronics Conference and Exposition (APEC)*, USA, Mar. 2016, pp. 2770-2775, doi: 10.1109/APEC.2016.7468256.
- [16] S. Gueye, L. Thiaw, M. F. Ndiaye, I. Ngom, M. Diop, and E. H. M. Ndiaye, "A sensorless speed control of DC motor based on an adaptive reference model," *4th Biennial International Conference on Nascent Technologies in Engineering (ICNTE)*, India, 2021, pp. 1-5, doi: 10.1109/ICNTE51185.2021.9487787.




- [17] K. Horvath, "Comparison of extended and unscented Kalman filters with and without using mechanical model for speed sensorless control of induction machines," *2023 18th Conference on Electrical Machines, Drives and Power Systems (ELMA)*, Bulgaria, 2023, pp. 1-4, doi: 10.1109/ELMA58392.2023.10202302.
- [18] M. Vidlak, L. Gorel, and P. Makys, "Performance evaluation, analysis, and comparison of the back-EMF-based sensorless FOC and stable V/f control for PMSM," *2022 International Symposium on Power Electronics, Electrical Drives, Automation and Motion (SPEEDAM)*, Italy, 2022, pp. 318-323, doi: 10.1109/SPEEDAM53979.2022.9842027.
- [19] J. Mohanalakshmi, and H. N. Suresh, "Sensorless speed estimation and vector control of an induction motor drive using model reference adaptive control," *2015 International Conference on Power and Advanced Control Engineering (ICPACE)*, India, Aug. 2015, pp. 377-382, doi: 10.1109/ICPACE.2015.7274976.
- [20] S. Dhundhara, P. Kumar, and Y. P. Verma, "Sensor less speed control of PMSM using space vector pulse width modulation based on MRAS method," *015 2nd International Conference on Recent Advances in Engineering & Computational Sciences (RAECS)*, India, Dec. 2015, doi: 10.1109/RAECS.2015.7453408.
- [21] Y. B. Zbede, S. M. Gadoue, and D. J. Atkinson, "Model predictive MRAS estimator for sensorless induction motor drives," *IEEE Transactions on Industrial Electronics*, vol. 63, no. 6, pp. 3511-3521, 2016, doi: 10.1109/TIE.2016.2521721.
- [22] P. Ramasamy, and V. Krishnasamy, "SVPWM control strategy for a three phase five level dual inverter fed open-end winding induction motor," *ISA Transactions*, vol. 102, pp. 105-116, 2020, doi: 10.1016/j.isatra.2020.02.034.
- [23] T. Araoye, E. C. Ashigwuike, A. C. Adeyemi, S. V. Egoigwe, N. G. Ajah, and E. Eronu, "Reduction and control of harmonic on three-phase squirrel cage induction motors with voltage source inverter (VSI) using ANN-grasshopper optimization shunt active filters (ANN-GOSAF)," *Scientific African*, vol. 21, 2023, doi: 10.1016/j.sciaf.2023.e01785.
- [24] Q. Tan, L. Mao, Y. Cai, B. Zhang, and Z. Ruan, "Comparative evaluation and analysis of GaN-based VSIs and CSIs," *Energy Reports*, vol. 9, no. 1, pp 568-576, 2023, doi: 10.1016/j.egy.2022.11.082.
- [25] F. Shiravani, P. Alkorta, J. A. Cortajarena, and O. Barambones, "An improved predictive current control for IM drives," *Ain Shams Engineering Journal*, vol. 14, no. 8, 2023, doi: 10.1016/j.asej.2022.102037.

BIOGRAPHIES OF AUTHORS






Moustapha Diop    holds a Ph.D. in Electrical Systems and Renewable Energies. He is currently Associate Professor in the Department of Science and Industrial Technology at the Higher Normal School of Technical and Vocational Education (ENSETP) at Cheikh Anta Diop University in Dakar, Senegal, and a permanent researcher in the Energy, Water, Environment and Industrial Processes Laboratory (L3EPI). His current research focuses on power converters, control and modeling systems, and renewable energies. He is the author or co-author of several papers, published in international scientific journals and conference proceedings. He can be contacted at email: moustapha17.diop@ucad.edu.sn.



Abdoulaye Kebe    is Professor in the Department of Science and Industrial Technology at the Higher Normal School of Technical and Vocational Education (ENSETP) at Cheikh Anta Diop University in Dakar, Senegal. He holds a Ph.D. in Physics from the University of Paris Sud in 2013, and a master's degree in Analysis, Design and Research in the Field of Engineering Technologies in Education (ACREDITE) at the University of Cergy Pontoise in 2016. His research is mainly oriented towards renewable energies. He is author of several publications in the field of energy conversion. He is currently Director of ENSETP. He can be contacted at email: abdoulaye.kebe@ucad.edu.sn.



Ibrahima Gueye    holds a Ph.D. in Automation, Production, Signal and Image, and Cognitive Engineering from the University of Bordeaux. Currently, He is an Associate Professor at the Higher National School of Technical and Vocational Education. In addition to his pedagogical activities, he is affiliated with the Energy, Water, Environment, and Industrial Processes Laboratory (L3EPI) at the Polytechnic Superior School of Dakar, where he collaborate with a team of researchers on the design of electronic systems involved in the energy chain of photovoltaic solar systems. His aim is to optimize the transfer of electrical energy produced and promote the local manufacturing of electronic systems. He can be contacted at email: ibrahima64.gueye@ucad.edu.sn.